RESEACRH ARTICLE

SYNTHESIS, CHARACTERIZATION AND THEORETICAL CALCULATION OF *4-(((1H-IMIDAZOL-2-YL)METHYLENE)AMINO)PHENOL*

Dilek ELMALI [1], *, Kader ÇITAK [2]

[1] Department of Chemistry, Faculty of Science, Eskişehir Technical University, Eskişehir, Turkey
[2] Department of Chemistry, Faculty of Science, Eskişehir Technical University, Eskişehir, Turkey

ABSTRACT

In this study, the Schiff base 4-(((1H-imidazole-2-yl)methylene)amino)phenol (3), has been synthesized and the structure of the compound was characterized by elemental analysis, FTIR, ^{1}H NMR, ^{13}C NMR, and UV-Vis spectroscopic techniques. The correlation between theoretical and experimental spectroscopy data was examined. The acidity constant was calculated by using the PM6 method in the MOPAC2012 program and the DFT method in Gaussian09 program at B3LYP/6-311+G(d,p) levels at gas and liquid phases at 25 °C. After deciding the stable conformation of the synthesized molecule, HOMO, LUMO, MEP, and SAS theory were calculated using the B3LYP / 6-311+g(d, p) level.

Keywords: Schiff Base, DFT, Theoretical Calculation, Stable conformation, pKa

1. INTRODUCTION

Schiff bases, N-substituted imine derivatives, are not only used in organic chemistry but also as ligands [1-3]. The first preparation of Schiff bases was reported in 1864 by H. Schiff [4]. Since then, various methods for the synthesis of Schiff bases have been described [5]. The simple imine derivatives are generally synthesized from the condensation of aldehyde and primary amines. Because Schiff base chemistry has organic, inorganic, organometallic, and complex (Bidentate, Tridentate, Tetradentate, and Polydentate Schiff's bases according to the bonds they make with the metal applications) it has found many common uses in polymer and drug chemistry [6-10]. It is known that Schiff bases, which have biological activity, have antibacterial and antitumor properties depending on their electron attracting or electron-donating groups [11-13].

In the literature, there is no information on the acidity constant of the molecule in this study. There is a close interest between the acidity constant and the structure, properties, tautomeric state, formation, and reaction of the substance. There are various methods for determining the acidity constants such as potentiometric titration, spectrophotometric determination, and conductivity. The Ultraviolet-Visible spectrophotometric method is the most widely used and most sensitive method among other methods for the determination of acidity constants. Although this method takes a lot of time, it is preferred because it requires few substances and is very sensitive [14]. Theoretical calculations are economical methods that can be applied without chemical consumption, where laboratory conditions can be adjusted. Due to its practicality and speed, theoretical studies have found many application areas.

In this study, the synthesis (Scheme 1) characterization of 3 substances, which are thought to have active drug properties, was synthesized by the method of obtaining similar compounds, although the same substance is not found in the literature. [15, 16]. The characterization of the synthesized structure was carried out and spectroscopic studies were supported by the DFT calculation method. To find the

acidity constant, the sum of the electronic and thermal Free Energy of the Schiff base was calculated using the DFT method in gas and aqueous medium at room temperature. The pKa of the molecule was calculated from the sum of the electronic and thermal Free Energy. Calculations were made in Gaussian09 program with the DFT method at B3LYP/6-311G(d,p) level and MOPAC2016.
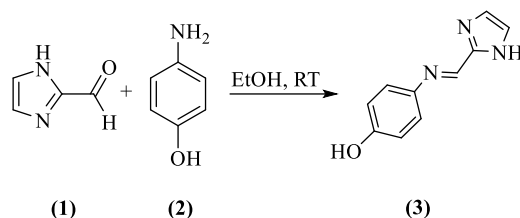
Scheme 1. Synthesis of 4-(((1H-imidazole-2-yl)methylene)amino)phenol (**3**).

2. EXPERIMENTAL SECTION

2.1. General Procedures

Melting points were taken with the Mettler-Toledo MP90 device. Infrared spectra were recorded in the range of 4000-400 cm^{-1} on a Perkin Elmer precisely Spectrum 100 FT-IR spectrometer using KBr disks for solid samples. ^{1}H-NMR and ^{13}C-NMR spectra were recorded on an Aligent 400 MHz DD2 spectrometer operating at 400.13 MHz for proton and at 100.62 MHz for carbon. ^{1}H NMR spectra were measured for ca. 25-30% solutions in DMSO-d$_6$ unless otherwise indicated and all chemical shifts are expressed relative to TMS (Me$_4$Si). Analytical thin-layer chromatography was carried out using aluminum-backed plates coated with Merck Kieselgel 60 GF254. UV-vis spectra were recorded with SHIMADZU UV-3150 UV-Visible spectrophotometer.

2.2. Synthesis

1H-imidazole-2-carbaldehyde (1 mmol) was dissolved in absolute ethanol (50 mL) and the temperature was raised to 60°C and stirring was continued at this temperature until the aldehyde dissolved [5]. Then 4-aminophenol (1 mmol) was added to the mixture. The entire mixture was stirred at room temperature and the progress of the reaction was monitored by TLC. The reaction mixture was poured onto crushed ice until a colored solid phase was formed. The separated solid product was filtered and recrystallized with ethanol.

2.2.1. *4-(((1H-imidazol-2-yl)methylene)amino)phenol (3)***:** This compound was obtained as brown powder (72%), mp 223 ºC; Anal. Calcd. for C$_{10}$H$_9$N$_3$O: C, 64.16; H, 4.85; N, 22.45; O, 8.55. Found: C, 63.30; H, 5.16; N, 21.61; O, 9.36. FT-IR (KBr, disk, ν cm-1): 3280 (O-H, N-H peak overlapped with O-H peak and remained below O-H peak), 3144-3069 (C-H, aromatic), 1621 (C=N), 1581-1444 (C=C, aromatic), 1247 (C-O) ^{1}H NMR (400 MHz, DMSO-d6) δ 12.93 (s, 1H phenol OH), 9.57 (s, 1H imidazole NH), 8.40 (s, 1H imine C=N), 7.22 (dd, J = 33.6, 24.9 Hz, 4H benzene), 6.80 (d, J = 8.7 Hz, 2H imidazole). ^{13}C NMR (101 MHz, DMSO-d$_6$) δ 156.90 (s), 147.66 (s), 145.71 (s), 142.36 (s), 130.83 (s), 122.89 (s), 120.14 (s), 116.23 (s).

3. THEORETICAL CALCULATIONS

3. 1. General Method

In the calculations for the molecule by using Intel(R) Core(TM) i5 X 3230M, 2.60 GHz, K55VD.411, 988B RPGA socket, X16 chipset workstation, (Marvin Beans, 2010 https://chemaxon.com/products/marvin) programs and CS ChemOffice Pro 12.0 for Microsoft Windows (CS ChemOffice Pro) and Gaussian 09 (Gaussian 09, 2009) program [17-20] the following calculation methods are used: Calculations with Gaussian 09 program were done with the DFT method, B3LYP

function and 6-311+g(d,p) basis set. In order to determine the most stable conformations of molecules, after drawing the molecules in the ChemDraw program, their stable conformations were calculated by transferring them to Marvin Beans (Marvin Beans, 2010 https://chemaxon.com/products/marvin)program. The calculated stable conformations of the molecule are minimized in the Chem3D program. The most stable conformations were calculated again by optimizing the molecule that was minimized in the Gaussian09 program with the "opt = mod redundant B3LYP/6-311+G(d,p)" in the DFT method. Thermodynamic results from the most stable conformations of molecule calculated were calculated with "freq B3LYP/6-311+G(d,p)".

The compound has been investigated with the Gaussian09 program by DFT method B3LYP/6-311+G(d,p) in vacuum and water phases. The UV-Vis spectra of the stable forms of the compounds have been determined and their electronic transition properties, the shifts depending on the solvents and the HOMO-LUMO (Highest Occupied Molecular Orbital- Lowest Unoccupied Molecular Orbital) values, Molecular Electrostatic Potentials (MEP) and Solvent Accessibility Surface (SAS) have been calculated.

3.2. Theoretical Calculation of pK$_a$

3.2.1. DFT method

The studied molecules were drawn with the ChemDraw Professional program [18] and the optimization of the molecules was performed with the Gaussian program [19]. Secondly, input files of molecules have been established in GaussView5 software [20]. In the last step, input files were created by using the B3LYP/6-311+G(d,p) [21-26] level of theory and transferred to the Gaussian09W packet program [19, 27] for calculation.

The acidity constants are directly related to the free energy of the deprotonation Reaction Equation 1.

$$AH \rightleftharpoons A^- + H^+ \qquad\qquad 1$$

and defined as given in Equation 2.

$$pK_a = \Delta G_R / 2.303\, RT \qquad\qquad 2$$

The deprotonation of a compound in an aqueous solution can be represented as a part of a thermodynamic cycle (Figure 1). Figure 1 explains the interrelationship between the gas and solution thermodynamic parameters [28, 29].
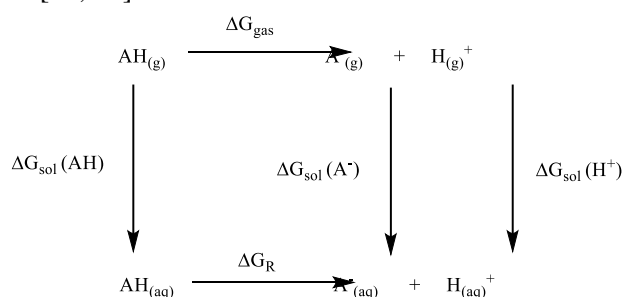

Figure 1. The interrelationship between the gas phase and solution thermodynamic parameters

One part of this cycle, ΔG_{gas} is the gas-phase deprotonation energy of the molecule. Three other parts ΔG_{sol} (AH), ΔG_{sol} (A$^-$), ΔG_{sol} (H$^+$) are the free energy of solvation of the protonated and deprotonated form of the molecule and the proton, respectively. The last part of the cycle ΔG_R,is the Sum of electronic and thermal Free Energies of deprotonation in solution and can be calculated as given in Equation 3.

$$\Delta G^o_{aq} = [\Delta G^o_s (A-) + \Delta G^o_s (H+) - \Delta G^o_s (AH)] + [\Delta G^o_g(A-) + \Delta G^o_g(H+) - \Delta G^o_g(AH)] \qquad 3$$

The total energies are given in Hartree's using the conversation factor 1 Hartree $=627.5095$ kcal mol^{-1}. The value of $\Delta G_{sol}(H^+)$ was taken as -48216.98 kcal mol^{-1} and $\Delta G_g(H^+)$ was taken as -48140.08 [30].

3.2.2. MOPAC method

For pKa calculation with Mopac program, MOPAC2016, Version: 17,039W was used. Since this program only calculates the pKa of hydroxyl hydrogens, the pKa value of the phenolic hydrogen (O-H) in the compound was calculated. In the calculation, the keywords "pm6 example of normal geometry definition debug ef charge=0", "oldgeo pm6 example of normal geometry definition debug ef charge=0", and "oldgeo pm6 gnorm=0.05 precise sparkle bfgs xyz pka let charge=0" used. Calculated pKa results are given in Table 7. http://openmopac.net/manual/pka.html

3.2.3. MarvinSketch method

Calculation of pKa with the MarvinSketch program was made using the version of MarvinSketch 20.6 (Marvin Beans, 2010 https://chemaxon.com/products/marvin). With this program, pKa values of nitrogen in the imidazole ring (CH = N), nitrogen in the imine group (CH = N), nitrogen-bound hydrogen in the imidazole ring (N-H), and oxygen-bound hydrogen in the phenol structure (O-H) were calculated. In the calculation, Mode: macro, Acid / base prefix: dynamic, Min basic pKa: -2, Max acidic pKa: 16 and Temperatura (K): 298 were selected [31]. The stacked pKa results are given in Table 7.

4. RESULTS AND DISCUSSION

4.1. Spectroscopic Results

4.1.1. UV-Vis spectroscopy

The UV spectrum of the studied molecule was taken between 190nm and 400nm in ethanol at room temperature as in the literature [32] (Figure 2). Generally, in the electronic absorption spectra of Schiff base compounds exhibit strong absorption bands at 266 nm. The band observed at 266 nm is the band belonging to the π-π * transition, which the band belonging to the n-π * transition to be observed was not observed because it was overlapped the broadband belonging to the π-π * transition.
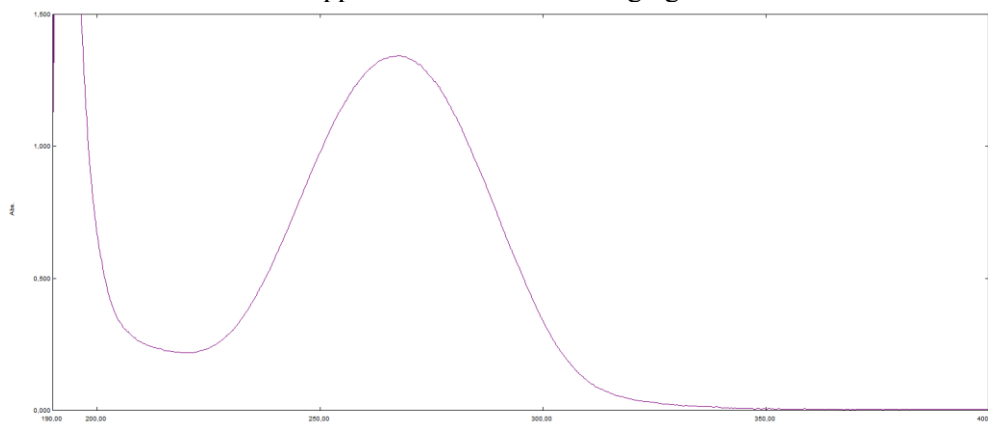

Figure 2. The experimental UV–Vis spectrum of molecule **3**.

Theoretically calculated UV spectrum with DFT B3LYP/6-311+G(d,p) is as in Figure 3. Since it was not in harmony with the experimental UV spectrum, the spectrum was taken again in buffer solutions prepared in notr (pH 7), acidic (pH 1), and basic (pH 13) buffer solutions experimentally. It was observed that the spectrum taken at pH 7 showed two peaks similar to the theoretically acquired spectrum (Figure 4)
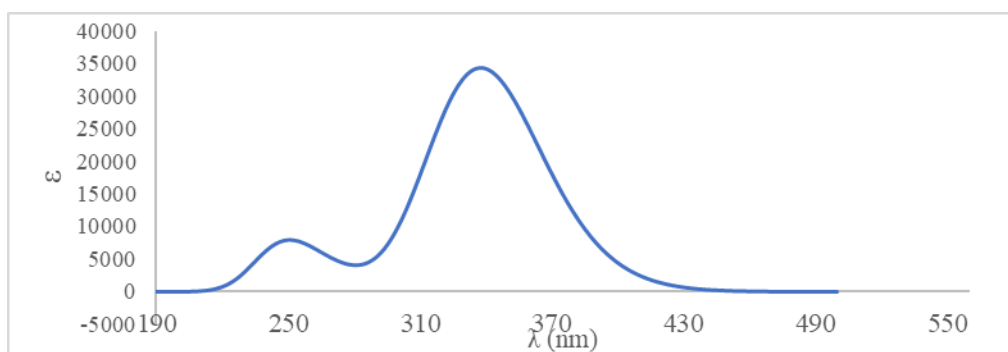
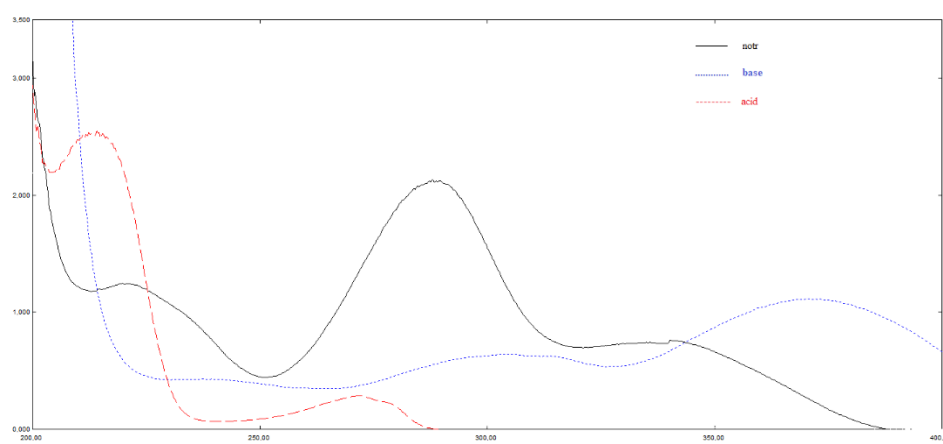**Figure 3.** The theoretical UV–Vis spectrum of molecule 3.

Figure 4. The experimental UV spectrum of molecule **3** in notr (pH 7), acidic (pH 1) and basic (pH 13) buffer solutions.

4.1.2. Vibrational spectroscopy (IR)

FT-IR spectra of molecule 3 was obtained using the KBr disk (Figure 5). The aromatic structure shows the presence of C–H stretching vibrations in the region 3144-3069 cm^{-1}, which is the characteristic region for ready identification of C–H stretching vibrations. The phenolic group O-H shows a stretching band in the 3280 cm^{-1} range. The C=C stretching peaks in the aromatic rings are observed between the 1581-1444 cm^{-1} range. The C-O stretching band of the phenol is found in the range of 1247 cm^{-1}. The C=N stretching frequency is found at 1621 cm^{-1}.The N-H peak that should be observed in the imidazole ring could not be observed because it overlapped the phenolic group O-H peak.
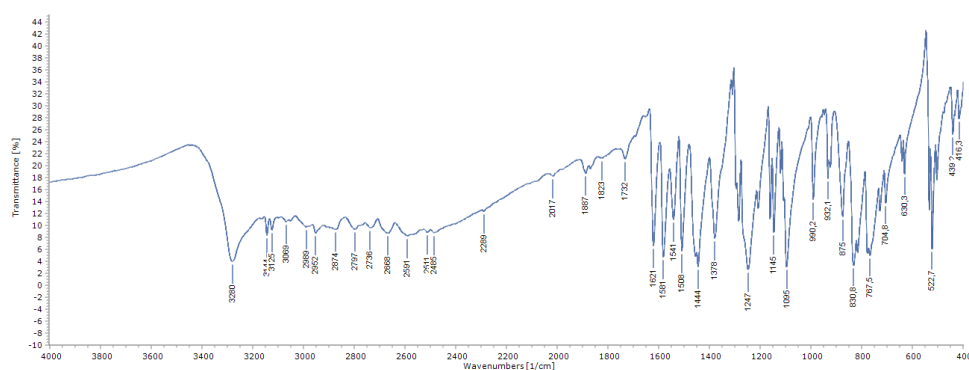

Figure 5. The experimental IR spectrum of molecule **3**

Theoretical infrared calculations of compound 3 were performed on the DFT B3LYP/6-311+G(d,p) base set. The Infrared Bands are visualized with the Gauss-View program and summarized in Table 1. Although the results obtained and the experimental data are generally in agreement, the experimental data. When the data were compared, it was determined that the theoretical values were insufficient. The main reason for this is that while there are intermolecular interactions in the experimental data, the theoretical calculations are carried out on a single molecule and the theoretical calculations are taken in the gas phase while the experimental data are taken in the solid state (Figure 6).
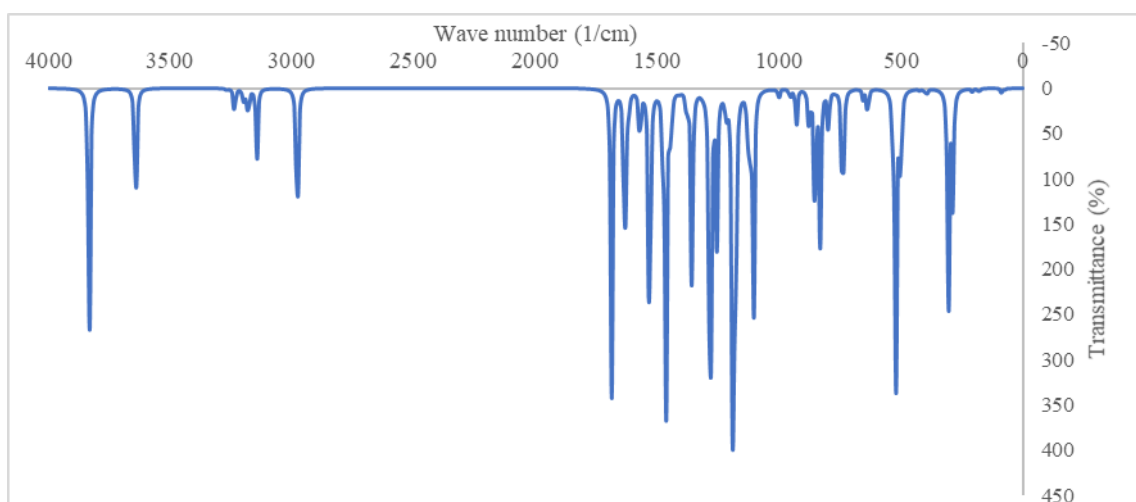

Figure 6: The theoretical IR spectrum of molecule **3**.

Table 1. The experimental and theoretical characteristic IR frequencies (cm^{-1}) of molecule **3**.

	Experimental ν(cm^{-1})	Theoretical ν(cm^{-1})
υ O-H (aromatic)	3280	3834.17
υ N-H (iminee)	Not observed (It was not observed because it remained below the O-H peak)	3643.24
υ C-H (aromatic imidazole ring)	3165 3144	3268.74 3237.34
υ C-H (aromatic benzene ring)	3125 3069 3051	3201.69 3187.41 3180.00 3145.50
υ N-H (imine)	2989	2979.52
υ C=N (imine)	1621	1688.37
υ C=C (benzene ring)	1581 1541 1508	1635.15 1620.62 1523.78
υ C=C (imidazole ring)	1455 1444	1572.50 1476.61 1465.20
υ C-O (aromatic)	1247	1283.62

The correlation of theoretical and experimental IR spectra was found to be 0.99 (Figure 7).
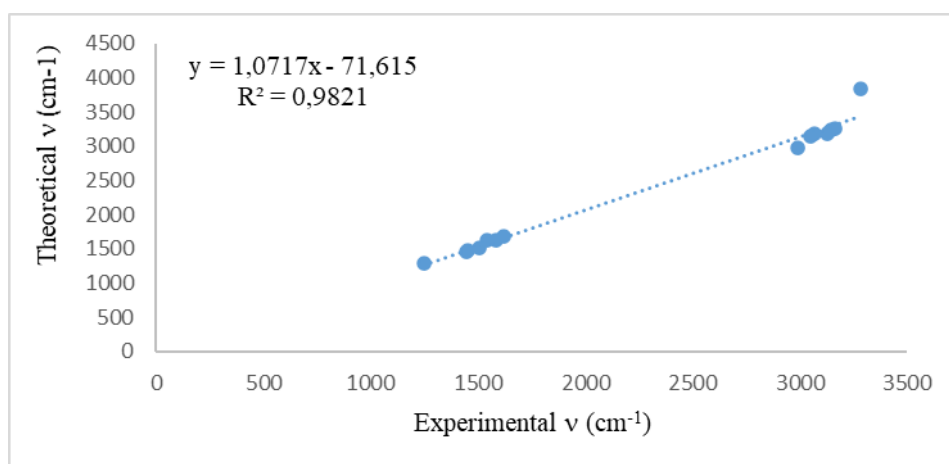
Figure 7. The correlation graph of the experimental and theoretical vibrational IR frequencies of molecule 3.

4.1.3. ^{1}H and ^{13}C nuclear magnetic resonance spectroscopy (NMR)

The experimental ^{1}H and ^{13}C NMR spectral data of the molecule are shown in Figure 8. The ^{1}H NMR spectrum of the Schiff base ligand was recorded in DMSO-d_6. In the ^{1}H NMR spectra of Schiff base ligand, the peaks appeared at 7.22 and 6.80 ppm were assigned to the proton of the phenolic group, singlet peaks appeared at 7.27 and 7.13 were assigned to the imidazole, and singlet peaks appeared at 8.40 ppm were assigned to protons of imine group. The ^{13}C NMR spectrum of the Schiff base ligand was recorded in DMSO-d_6. In the ^{13}C-NMR spectra of the molecule, the signal that appeared at 156.90 ppm was assigned to imine carbon atoms (C=N). A signal at 147.66, 145.71, 122.89, and 116.23 ppm were assigned for phenolic carbon. The carbons of the imidazole were observed at 142.36, 130.83, and 120.14 ppm.
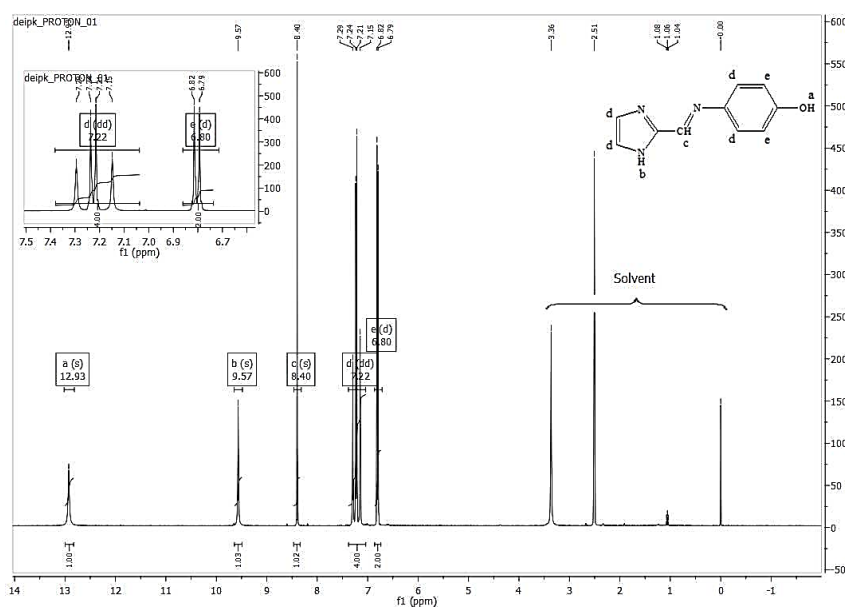
(a)
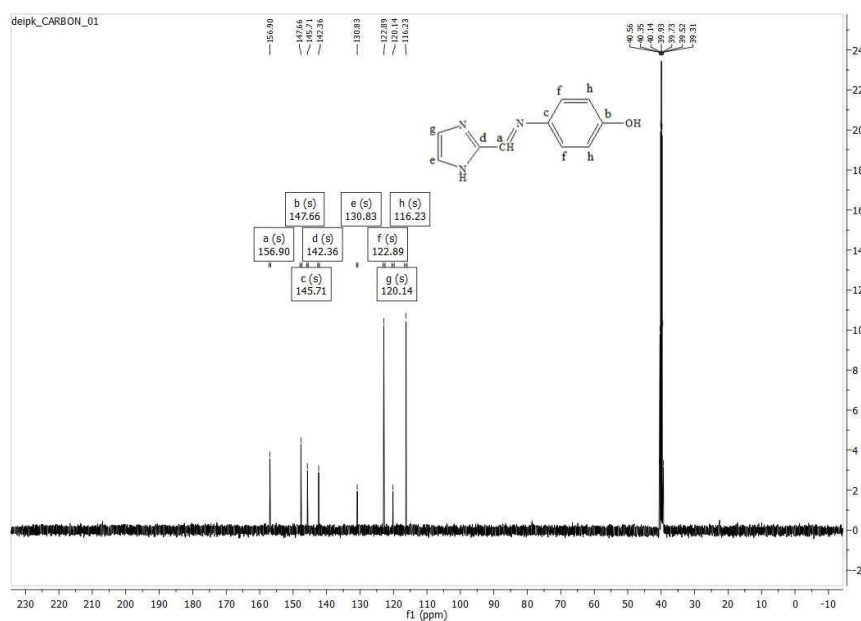
(b)

Figure 8. ^{1}H (a) and ^{13}C (b) NMR spectra of molecule **3** in DMSO- d_6 were obtained experimentally.

Experimental NMR analysis was taken in 400 MHz NMR device in DMSO-d6 solvent environment, and theoretical NMR analysis was taken in B3LYP / GIAO model set and the values were summarized in Table 2 and Table 3. When the experimental and theoretical NMR values are compared, the equation at ^{1}H-NMR is y = 1,1276x-1,0639; R^2 = 0,5954 while in ^{13}C-NMR the equation is y = 0,6923+56,321; R^2 = 0.4326. When R^2 values are examined, bad harmony is observed in theoretical and experimental values; It can be said that this value in ^{1}H-NMR is lower since acidic protons are more mobile than other protons.

Table 2. ^{1}H chemical shifts δ [ppm] determined as experimental and theoretical for molecule **3**.

Theoretical		Experimental	
Atom	Chemical Shift	Atom	Chemical Shift
20H	3.99	a (1H, s)	12.93
21H	8.43	b (1H, s)	8.40
15H	8.98	c (1H, s)	9.57
16H 19H 22H 23H	8.06 7.81 7.26 7.75	d (4H, dd)	7.22
17H 18H	7.32 6.71	e (2H, d)	6.80

Table 3. ^{13}C NMR chemical shifts δ [ppm] determined as experimental and theoretical for molecule **3**.

Experimental		Theoretical	
Atom	Chemical Shift	Atom	Chemical Shift
C2	156.90	a (s)	150.47
C7	147.66	b (s)	175.16
C4	145.71	c (s)	1 58.71
C1	142.36	d (s)	162.88
C12	130.83	e (s)	131.31
C5 C9	122.89	f (s)	153.59 127.60
C13	120.14	g (s)	150.91
C6 C8	116.23	h (s)	131.99 128.12

4.2. Theoretical Results

4.3. Energy, Dipole and Mulliken Atomic Charge Values

Dipole moment, polarization, and acid-base behavior of a molecule are affected by atomic charges. Therefore Mulliken atomic charge calculations play an important role in chemical calculations. The Mulliken atomic charges were listed in Table 5. Accordingly, the most negative atom observed as oxygen bound to the benzene ring. Although, usually, heteroatoms and the carbon atoms attached to them are determined negatively, the most positive atom is in the benzene ring observed as the numbered nine carbon atom.

Dipole moment is an important parameter in chemistry and shows charge transfer across the molecule. Dipole moment for **3** was calculated as 6.031 D (Table 4). If the net dipole moment is greater than zero, the bond and molecule are considered polar. They tend to form chemical bonds with atoms that have similar electronegativity values.
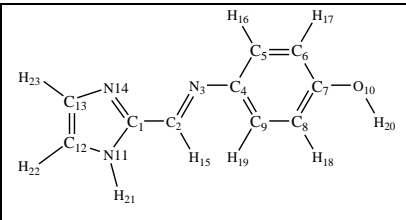
Zero-point energy is the lowest energy a physical system can have in quantum mechanics. Zero-point energy of the molecule determined 110,527 kcal/mol and Sum of electronic and thermal Free Energies determines -392800,817 kcal/mol.

Table 4. The zero-point energy, thermal free energies, and dipole moment of molecule **3**.

Zero-point vibrational energy (Kcal/Mol)	110,527
Sum of electronic and thermal Free Energies* (Kcal/Mol)	-392800,817
Dipole moment (Debye)	6,031

*1 Hatree=627.509 kcal/Mol

Table 5. The Mulliken atomic charges of molecule **3**.

Atom	Mulliken atomic charges
1C	-0.136
2C	-0.253
3N	0.096
4C	-0.333
5C	-0.216
6C	-0.022
7C	-0.491
8C	-0.170
9C	0.359
10O	-0.230
11N	-0.113
12C	-0.230
13C	0.240
14N	-0.130
15H	0.068
16H	0.209
17H	0.196
18H	0.150
19H	0.104
20H	0.265
21H	0.284
22H	0.165
23H	0.186

4.3.1. pK$_a$ Calculation

Formation enthalpies of the cis and trans forms of the molecule were calculated (Figure 9). Since the formation enthalpy of cis form is very high, we decided to make the pKa calculations on trans form. We calculated the acidity constant in trans form with the lowest energy dihedral angle.
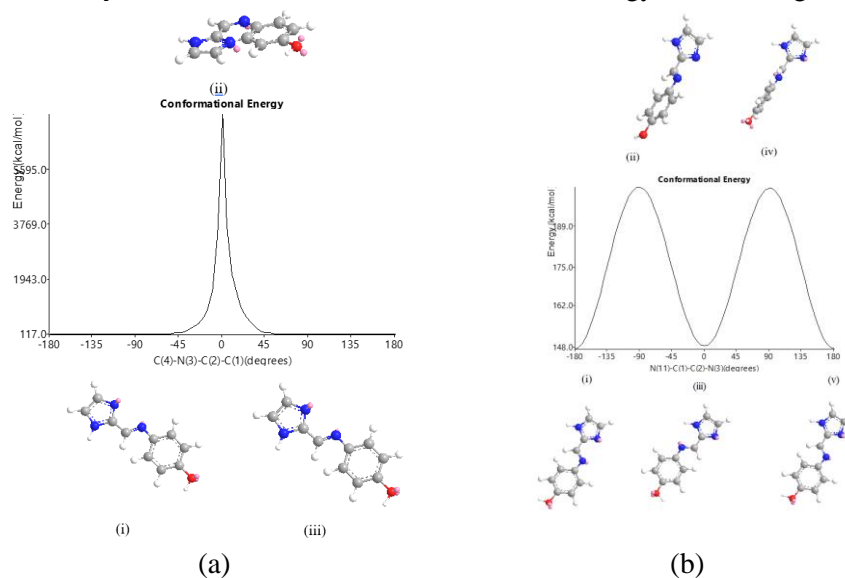

Figure 9. Calculated lowest energy dihedral angle graphics of the studied molecule's cis (a) and trans (b) forms.

Theoretical acidity constants have been made by considering the protonation and deprotonation center (Figure 10) of the molecule were calculated in the Gaussian09 program at the level of DFT method B3LYP/6-311++G(d,p) according to equation 3 (Table 6) [33].
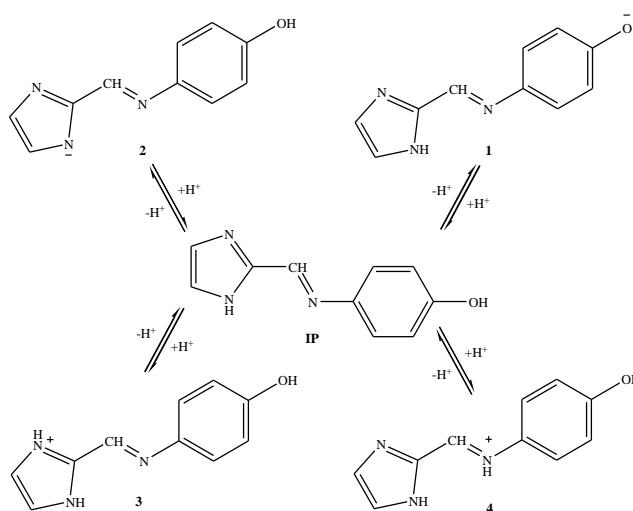

Figure 10. The protonated and deprotonated forms of the studied molecule are shown in the Scheme.

Table 6. The calculated pK_a values of the molecule **3**

Molecule	BH⁺s	Bs	BH⁺g	Bg	ΔGs	ΔGg	δΔG(BH⁺)	pKa calc.
1	-392671.493	-392367.041	-392656.924	-392310.175	-68.632	-182.030	-250.662	2.2643
2	-392675.164	-390298.145	-392665.648	-390242.205	-2141.199	-2258.723	-4399.922	3.5087
3	-392963.744	-392671.493	-392916.720	-392656.924	-56.431	-95.076	-151.506	2.0457
4	-392960.689	-392671.493	-392913.094	-392656.924	-53.376	-91.450	-144.825	2.0261

Deviation= Experimental pK_a- Calculated pK_a

Values of pKa were predicted using MarvinSketchTM 5.3.7 (ChemAxon Ltd., Budapest, Hungary; www.chemaxon.com) and MOPAC2016. The fact that the MOPAC2016 calculations are compatible with the 1 data from different conformations made for MarvinSketch (ChemAxon), shows that these methods are in harmony. The theoretically were calculated pK_a values of the molecule studied are given in Table 7.

Table7. The calculated pK_a values of the molecule **3**

Molecule 3	Method	pKa
A	MOPAC2016	8.244
A		8.019
B	MarvinSketch	11.746
C		5.588
D		0.403
A		2.2643
B	DFT	3.508
C		2.045
D		2.026

4.3.2. HOMO-LUMO

The Highest Occupied Molecular Orbital (HOMO) and the Lowest Unoccupied Molecular Orbital (LUMO) play a key role in the determination of molecular properties [34]. HOMO-LUMO energy values and energy maps represent the chemical activity and kinetic stability of the molecule. HOMO and LUMO surfaces and energies of the molecule was calculated in the gas phase and B3LYP/6-311+G(d,p) level in different solvents and the results obtained are given in Figure 11. When the HOMO values of the obtained compound were examined, it was determined that the electron density was distributed over the whole compound.
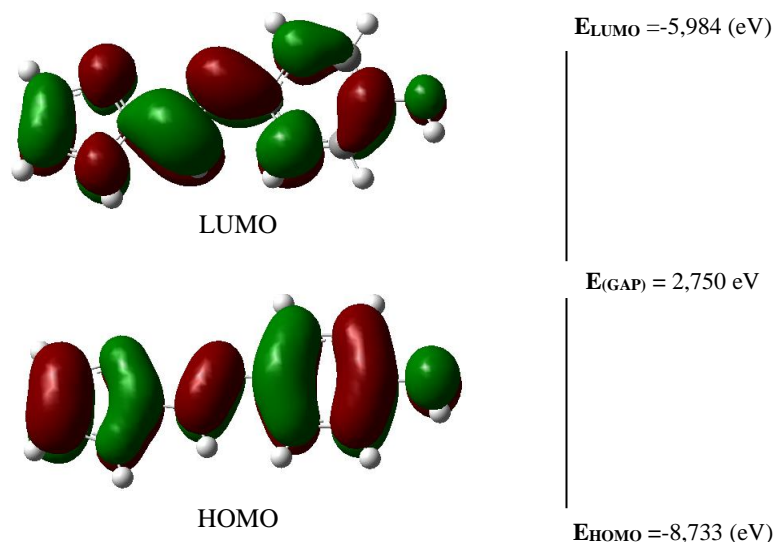

E_{LUMO} = -5,984 (eV)

$E_{(GAP)}$ = 2,750 eV

E_{HOMO} = -8,733 (eV)

Figure 11. HOMO and LUMO 3D plots of molecule 3 were obtained with the B3LYP/6-311 + g(d, p) method.

Chemical hardness and softness are important parameters for the stability and reactivity of the molecule. Hard molecules have large energy values soft molecules have small energy values. Soft molecules are more reactive than hard molecules because they can easily present their electrons to a receptor. Other molecular parameters can be associated with these values. Accordingly, the low HOMO-LUMO values of the obtained compound indicate that the reaction activity will be easier and it can easily bind to metal atoms or a receptor.

4.3.3. Molecular electrostatic potential (MEP) surface analysis

The Molecular Electrostatic Potential (MEP) is an optical method that provides information about the net electrostatic effect created by the total charge distribution in the molecule, as well as the electronegativity of a compound, its charge, dipole moment, and its ratio to the chemical reaction while allowing us to understand the molecular polarity [35]. The different colors of the resulting compound dimensionally are shown in the MEP map. In colors, the blue color indicates positive regions of the molecule, green color indicates mild regions and red color indicates negative regions. The MEP surface of the molecule was plotted using the 6-311 + G(d, p) based DFT / B3LYP level adjusted to estimate the reactive sites of the electrophilic and nucleophilic attack on the molecule investigated (Figure 12). According to this, the regions of the compound, especially the regions where oxygen and nitrogen atoms are rich in electrons, are the places where hydrogen atoms are seen as positive.
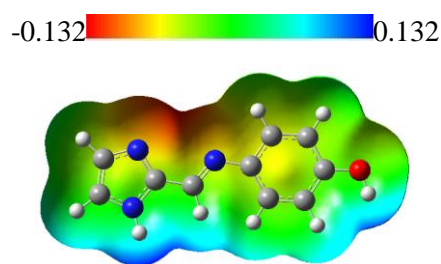
-0.132 ▮ 0.132

Figure 12. MEP 3D plot of molecule 3 obtained with B3LYP/6-311 + g(d, p) method.

4.3.4. Solvent Accessibility Surface (SAS)

The solvent accessibility surface of the compound is given in Figure 13. SAS, showing regions of interaction with the solvent, is very useful for describing specific solute-solvent interactions. The red regions indicate the regions where polar or polar protic solvents will interact with the oxygen atom in the compounds. The blue regions indicate the regions where polar or polar protic solvents will interact with the nitrogen atom in the compounds. Green regions indicate the regions where polar or polar protic solvents will interact with the -Cl atom in the compound. Gray regions indicate the regions where apolar solvents will interact with benzene rings and other saturated hydrocarbons in the compound. Compounds appear to interact with polar or polar protic solvents, polar atoms (N, O, and S), and apolar solvents with low polarity atoms (C).
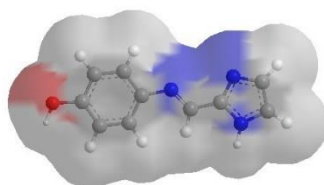

Figure 13. MEP 3D plot of molecule 3

4.3.5. Dielectric Constant

The dielectric coefficient (dielectric constant) can be defined as the ratio of the permittivity of the medium to the permittivity of the free space. Permeability is the quality that describes the effect of a material on an electric field. The higher the permeability, the more the material tends to reduce the area created in that area. Materials with a high dielectric constant have a strong ability to become polarized. If the polarization developed by applying an electric field is high for a dielectric material, the dielectric constant will also be high. The higher the resistance to electric current flow, the higher the dielectric constant.

For this molecule, the isoelectric point was found to be 6.92 as a result of the calculations we made in the Marven program.

5. CONCLUSION

In this study, the synthesis of 4-(((1H-imidazole-2-yl)methylene)amino)phenol (IP) compound was performed for the first time in the literature. The structure of the obtained compound was illuminated by ^{1}H-NMR, ^{13}C-NMR, IR, UV-Vis, and elemental analysis techniques. In the second stage of the study, the theoretical calculations of the compound were made with the Gaussian 09 program. Experimental and theoretical IR and UV-Vis values were generally in harmony.

We aimed to contribute with theoretical studies, thinking that the synthesized structure could be used as a drug in future studies. One of the most important factors in the attachment of a molecule to a biological target is its conformation. For this reason, all theoretical studies have been based on the lowest energy conformation. The acid-base dissociation constant (pKa) of a drug is an important physicochemical parameter that affects many biopharmaceutical properties. The pKa distributions of drugs are affected by two main factors. The first relates to the nature and frequency of formation of functional groups commonly observed in pharmaceuticals and the typical range of pKa values they emit. The other factor has to do with the biological targets these compounds are designed to hit. Determination of the pKa value in terms of examining the active drug property of the synthesized structure in this study was determined theoretically because it is important for future studies. Since its conductivity is 6.92, it was thought that the studied material could be used as an insulator.

ACKNOWLEDGMENTS

CONFLICT OF INTEREST

The authors stated that there are no conflicts of interest regarding the publication of this article.

REFERENCES

[1]   Yamada S. Advancement in stereochemical aspects of Schiff base metal complexes. Coordination Chemistry Reviews 1999; 190–192; 537–555.

[2]   Archer RD, Wang B. Synthesis and Characterization of the Thermally Stable Copolymer of Tetrakis(salicylaldehydato-O.O')zirconium(IV) and 3.3'-Diaminobenzidine. Inorg Chem, 1990; 29, 39-43.

[3]   Issa RM, Khedr AM and Rizk H. ^{1}H NMR IR and UV/VIS Spectroscopic Studies of Some Schiff Bases Derived From 2-Aminobenzothiazole and 2-Amino-3-hydroxypyridine. Journal of the Chinese Chemical Society, 2008; 55, 875-884.

[4]   Blagus A, Cinčić D, Friščić T, Kaitner B, Stilinović V. Schiff bases derived from hydroxyaryl aldehydes: molecular and crystal structure. tautomerism. quinoid effect. coordination compounds. Maced J Chem and Chem Eng, 2010; 29(2), 117-138.

[5]   Aytekin TM, Elmalı D, Berber H, Şişman F. Synthesis, characterization, crystal structure and theoretical studies of n-(2,4-dichlorobenzylidene)-3-methylbenzenamine, Anadolu University Journal of Science and Technology A- Applied Sciences and Engineering 2016; 17(2), 357 – 376.

[6]   Sridhara SK, Saravanana M, Ramesh A. Synthesis and antibacterial screening of hydrazones. Schiff and Mannich bases of isatin derivatives. Eur J Med Chem, 200; 36, 615–625.

[7]   Govındaraj V. Ramanathan S. Synthesis. spectral characterisation. electrochemical. and fluorescence studies of biologically active novel Schiff_ base complexes derived from E-4-(2-hydroxy-3- methoxybenzlideneamino)-N-(pyrimidin-2-yl)benzenesulfonamide. Turk J Chem, 2014; 38, 521-530.

[8]   Mladenova R, Ignatova M, Manolova N, Petrova T, Rashkov I. Preparation characterization and biological activity of Schiff base compounds derived from 8-hydroxyquinoline-2-carboxaldehyde and Jeffamines ED. European Polymer Journal, 2002; 38; 989–999.

[9]   Rousso I. Friedman N. Sheves M. Ottolenghi M. PKa of the Protonated Schiff Base and Aspartic 85 in the Bacteriorhodopsin Binding Site Is Controlled by a Specific Geometry between the Two Residuest. Biochemistry, 1995; 34, 37, 12059-12065.

[10]   Pradhan A and Kumar A. A Review: An Overview on Synthesis of Some Schiff bases and there Metal Complexes with Anti-Microbial Activity. Chemical and Process Engineering Research, 2015; 35; 2225.

[11]   Rousso I, Friedman N, Sheves M, Ottolenghi M. pKa of the Protonated Schiff Base and Aspartic 85 in the Bacteriorhodopsin Binding Site Is Controlled by a Specific Geometry between the Two Residuest. Biochemistry, 1995; 34; 12059- 12065.

[12]   Zhang X, Bı C, Fan Y, Cuı Q, Chen D, Xıao Y and Dou QP. Induction of Tumor Cell Apoptosis By Taurine Schiff Base Copper Complex is Associated the with İnhibition of Proteasomal Activity. Int J Mol Med, 2008; 5, 677–682.

[13]   Cinarli A, Gürbüz D, Tavman A and Birteksöz AS. Synthesis Spectral Characterizations and Antimicrobial Activity of Some Schiff Bases of 4-Chloro-2-Aminophenol. Bull Chem Soc Ethiop, 2011; 25(3), 407-417.

[14]   Sridhar G, Bilal I, Easwaramoorth D, Ran S, Kumar B and Manohar CS. Synthesis Characterization and Antimicrobial Activities of Copper Nickel Cobalt Chromium Complexes Derived from (Z)-4-Fluoro-N-(2.7-dimethylhept-6-enylidene) benzenamine. J. Braz. Chem. Soc., 2017; 28(5) 756-767.

[15]   Demir HÖ, Kaya I and Saçak M. Synthesis and characterization of a pyridine containing Schiff base oligomer Russian Chemical Bulletin. International Edition, October, 2006; 55(10), 1852-1855.

[16]   Radi S, Tighadouini S, Feron O, et al. One pot synthesis antitumor antibacterial and antifungal activities of some schiff base heterocycles . Int J Pharm, 2015; 5(1); 39-45.

[17]   CS ChemOffice Pro for Microsoft Windows.

[18] ChemBioDraw Ultra 14 Individual ASL SN Win. Download Individual Two Year Term English Windows. 2014.

[19]   Gaussian 09. Revision B.01. Frisch MJ, Trucks GW, Schlegel HB et al. Gaussian. Inc. Wallingford CT. 2009.

[20]   Dennington RD. Keith TA. Millam JM. GaussView 5.0.8. Gaussian Inc. Wallingford CT 2008.

[21]   Berber H, Uysal ÜD. Bazı diimin türevi schıff bazlarının sentezi, geometrileri ve tautomer yapılarının kararlılıklarının dft yöntemi ile hesaplanması, Anadolu University Journal of Science and Technology B- Theoretical Science, 2015; 3(2) 105 – 126.

[22]   Vidal Salgado LE, Vargas Hernández C. Spectrophotometric Determination of the pKa. Isosbestic Point and Equation of Absorbance vs. pH for a Universal pH Indicator. American Journal of Analytical Chemistry, 2014; 5, 1290-1301.

[23]   Casasnovas R, Ortega-Castro J, Frau J, et al. Theoretical pKa Calculations with Continuum Model Solvents. Alternative Protocols to Thermodynamic Cycles. International Journal of Quantum Chemistry, 2014; 114, 1350–1363.

[24]   Pliego JR, Riveros JM. Theoretical Calculation of pKa Using the Cluster-Continuum Model. J. Phys. Chem. A 2002; 106, 7434-7439.

[25]   Hohenberg P. Kohn W. Inhomogeneous Electron Gas. Phys. Rev.1964; B864,136.

[26]   Thapa B and Schlegel HB. Density Functional Theory Calculation of pKa's of Thiols in Aqueous Solution Using Explicit Water Molecules and the Polarizable Continuum Model. J. Phys. Chem. A 2016; 120, 5726−5735.

[27]   Perez-Jorda JM, Becke AD. A density-functional study of van der Waals forces: rare gas diatomics. Chemical Physics Letters 1995; 233, 134-137.

[28]   Stratmann RE, Scuseria GE, Frisch MJ. Achieving linear scaling in exchange-correlation density functional quadratures. Chemical Physics Letters 1996; 257, 213-223.

[29]   Hwang S and Chung DS. Calculation of the Solvation Free Energy of the Proton in Methanol. Bull. Korean Chem. Soc. 2005; 26 (4), 589-593.

[30]   Tawa G J, Topol IA, Burt SK et al. Calculation of the aqueous solvation free energy of the proton Citation: The Journal of Chemical Physics 1998;109, 4852.

[31]   Yıldırım A, Kaya Y, Göker M, Screening of simple carbohydrates as a renewable organocatalyst for the efficient construction of 1,3-benzoxazine scaffold. Carbohydrate Research, 2021, 510, 108458.

[32]   Türkoğlu G, Berber H, Dal H, Öğretir C. Synthesis, characterization, tautomerism and theoretical study of some new Schiff base derivatives, Spectrochimica Acta Part A 79, 2011; 1573–1583

[33]   Bruice TC, Schmir GL, Imidazole Catalysis I The Catalysis of the Hydrolysis of Phenyl Acetates by Imidazole, J. Am. Chem. Soc.*,* 1957; 79 (7), 1663–1667

[34]   Bahgat K, Fraihat S. Normal coordinate analysis, molecular structure, vibrational, electronic spectra and NMR investigation of 4-Amino-3-phenyl-1H-1,2,4-triazole-5(4H)thione by ab initio HF and DFT method. Spectrochimica Acta Part A: Molecular and Biomolecular Spectroscopy, 2015; 135, 1145-1155.

[35]   Bouabdallah I, Rahal M, Harit T, et al. Hartree-Fock and density functional theory studies on tautomerism of 5,5-diisopropyl3,3-bipyrazole in gas phase and solution. Chemical Physics Letters, 2013; 588, 208-21